

## Supporting Information

### **An effective modulation of bulk perovskite by V<sub>2</sub>CT<sub>x</sub> nanosheet for efficient planar perovskite solar cells**

Chen Tian<sup>1,2#</sup>, Yajie Yan<sup>3#</sup>, Shanglei Feng<sup>1,2#</sup>, Jiaou Wang<sup>4</sup>, Yingchun Niu<sup>5</sup>, Xiaoxi Li<sup>3</sup>, Huanxin Ju<sup>6</sup>, Quan Xu<sup>5</sup>, Yang Huang<sup>7</sup>, Hua Dong<sup>8</sup>, Ziqi Liang<sup>3</sup>, Bitao Dong<sup>\*9</sup>, Lina Li<sup>\*1,2</sup>, Yingguo Yang<sup>\*1,2,3</sup>

<sup>1</sup> Shanghai Synchrotron Radiation Facility (SSRF), Zhangjiang Lab, Shanghai Institute of Applied Physics & Shanghai Advanced Research Institute, Chinese Academy of Sciences, Shanghai 201204

<sup>2</sup> University of Chinese Academy of Sciences, Beijing 100049, China

<sup>3</sup> School of Microelectronics, Fudan University, Shanghai 200433, China.

<sup>4</sup> Institute of High Energy Physics, Chinese Academy of Sciences, Beijing 100049, China.

<sup>5</sup> State Key Laboratory of Heavy Oil Processing, China University of Petroleum-Beijing, 102249, China.

<sup>6</sup> PHI China Analytical Laboratory, CoreTech Integrated Limited, 402 Yinfu Road, Nanjing 211111, China.

<sup>7</sup> College of Materials Science and Engineering, Shenzhen University, Shenzhen 518055, China

<sup>8</sup> Key Laboratory for Physical Electronics and Devices of the Ministry of Education & Shaanxi, Xi'an Jiaotong University, China.

<sup>9</sup> Department of Chemistry, Ångström Laboratory, Uppsala University, Box 523, SE-751 20 Uppsala, Sweden.

#These authors (Chen Tian, Yajie Yan and Shanglei Feng) contribute equally to this paper.

\*Correspondence and requests for materials should be addressed to bitao.dong@kemi.uu.se (B.D.); lilina@sinap.ac.cn (L.L.); yangyingguo@sinap.ac.cn (Y.Y.).

## Experimental

**Materials:** Formamidinium iodide (FAI, 99.99%), Lead iodide (PbI<sub>2</sub>, 99.99%), 2,2',7,7'-tetrakis-(N,N-di-*p*-methoxyphenylamino)-9,9'-spirobifluorene (Spiro-OMeTAD), Anhydrous dimethyl sulfoxide (DMSO, anhydrous), chlorobenzene (CB) and *N,N*-dimethylformamide (DMF, anhydrous) were purchased from Sigma Aldrich. MABr, MAI, CsI were purchased from Xi'an Polymer Light Technology Corp.

**Synthesis of V<sub>2</sub>C<sub>x</sub> MXene:** 0.5g V<sub>2</sub>AlC (>92 wt%, Aladdin reagent Co., China) was added into a 150 mL plastic beaker, and 10mL 24% HF (Aladdin Reagent Co., China) was dropwise added while stirring under ice bath conditions. Then it was stored at 30°C for 56 h. Afterwards, the obtained suspension was repeatedly washed with deionized water until pH was 6-7, and then centrifuged to separate black precipitate. Finally, multi-layer V<sub>2</sub>C MXene was obtained by freeze-drying overnight at -40°C.

**Solution Preparation:** The SnO<sub>2</sub> precursor solution is prepared by mixing the SnO<sub>2</sub> colloid (15 wt.%, ~5 nm, Alfa Aesar) and deionized water in ratio of 1:4. The Cs<sub>0.042</sub>FA<sub>0.763</sub>MA<sub>0.195</sub>PbI<sub>0.928</sub>Br<sub>0.056</sub>Cl<sub>0.016</sub> precursor solution (263.114mg FAI, 783.7mg PbI<sub>2</sub>, 9.517g MABr, 22.083mg CsI and 20mg MAI dissolved in DMF: DMSO (4:1, v/v) mixed solvent) is prepared in a N<sub>2</sub> glove box and stirred at 50°C over 3h and then filtered through PTFE filters (0.22 μm) before usage. The V<sub>2</sub>C-CB solution is prepared by mixing V<sub>2</sub>C MXene and CB solution (0.005mg/mL, 0.010mg/mL, 0.015mg/mL and 0.020mg/mL) and then also filtered through PTFE filters (0.22 μm) before usage. Spiro-OMeTAD solution was prepared by mixing 22 μL lithiumbis

(trifluoromethanesulfonyl) imide (TFSI-Li) solution (520 mg Li-TFSI in 1 mL acetonitrile) and 36  $\mu$ L 4-tertbutylpyridine with 90 mg Spiro-OMeTAD in 1 mL CB solution.

**Device Fabrication:** Patterned ITO substrates were thoroughly cleaned in ultrasonic bath using acetone, ethanol, and deionized water in sequence for 20 min, respectively. SnO<sub>2</sub> electron transfer layer was spin coated onto the ITO substrates at 4000 rpm for 30 s and then annealed at 150 °C for 20 minutes in air. The perovskite film is prepared by a one-step spin-coating process. After the Perovskite precursor solution was spin coated onto the SnO<sub>2</sub> layer at 1000 rpm for 10 s and 4000 rpm for 30s, the mixed solution of V<sub>2</sub>C-CB solution or CB solution were dripped on the precursor films during the spin-coating process for another 15 s. Subsequently, the precursor film was annealing at 100 °C for 10 min and 150 °C for 15 min in nitrogen glove box to obtain the perovskite layer. To fabricate the PSCs, the solution of spiro-OMeTAD was spin-coated onto the perovskite layer at 5000 rpm for 30 s without annealing. Afterwards, the devices were placed in a drying cabinet for 24h to oxidize the surfaces. Finally, the device was transferred to a vacuum chamber at  $2 \times 10^{-6}$  Torr for Ag electrode evaporation. The active area of each device is 0.075 cm<sup>2</sup> as determined by the shadow mask.

**Characterization:** The light J–V curves were measured on a Keithley 2400 source meter unit under AM 1.5G light illumination with a Newport-Oriel (Newport, Class AAA solar simulator, 94023A-U) solar simulator operating at an intensity of 100 mW cm<sup>2</sup>. The light intensity was calibrated by a certified Oriel reference cell (91150V) and

verified with a NREL calibrated, filtered silicon diode (Hamamatsu, S1787-04). The devices were measured both in reverse scan (1.2 V/s-0.05 V, step 0.01 V) and forward scan (-0.05 V/s 1.2 V, step 0.01 V) with 0.06 V/s scan rate. The active area was determined by the aperture shade masks 0.075 cm<sup>2</sup>. The field-emission scanning electron microscope (SEM) images were obtained from ZEISS GeminiSEM300. Transmission electron microscope (TEM) images were taken from a FEI Tecnai G2F20 microscope. Atomic force microscopy (AFM) images were observed on a Bruker Nano Surfaces Division AFM. UV-vis absorption spectra were acquired on a Shimadzu UV-2700 spectrophotometer over the 200-900 nm wavelength range. Steady state photoluminescence (PL) spectra were taken on a fluorescence spectrophotometer (Fluoromax 4, HORIBA Jobin Yvon, United States). Time-resolved photoluminescence (TRPL) spectra were obtained using a streak camera (Hamamatsu, C6860). The laser source is an amplified titanium/sapphire laser providing 800 nm 35-fs pulses at 2 kHz which is then frequency doubled for 400 nm excitation. The X-ray diffraction (XRD) shown in Fig.1B was performed at the BL17B beamline of the Shanghai Synchrotron Radiation Facility (SSRF) using X-ray with a wavelength of 1.24 Å in transmission mode. The grazing-incidence wide-angle X-ray scattering (GIWAXS) measurements shown in Figs.3A and B were performed at the BL14B1 beamline of the SSRF using X-ray with a wavelength of 0.6887 Å. Two-dimensional (2D) GIWAXS patterns were acquired by a MarCCD mounted vertically at a distance ~423 mm from the sample with a grazing incidence angle of 0.2° or 0.4° and an exposure time of 5 sec. The standard sample used was lanthanum hexaboride (LaB<sub>6</sub>), which is

mainly used to determine the center of the circle and test distance. The software used for integrating 1D data shown in Figs.3A and B is FIT 2D and displayed in scattering vector  $q$  coordinates. The software used for exporting 2D graphs shown in Figs.3C and D is q2D. GIWAXS measurements shown in Figs.2J-K and Figs.S6 were performed at the BL17B beamline of the SSRF using X-ray with a wavelength of 1.24 Å. 2D GIWAXS patterns were acquired by a Platus2M detector mounted vertically at a distance  $\sim 300$  mm from the sample with a grazing incidence angle of  $0.4^\circ$ . The standard sample used was  $\text{LaB}_6$  too. The 2D GIWAXS data and 1D GIWAXS data were analyzed using the Matlab to run a program and Dioptas software, respectively. The SCLC characterization was scanned from 0 to 7V by Keithley 2636B source meter unit. Soft X-ray absorption spectroscopy(sXAS) was measured at 4B7B beamline of BSRF. Ultraviolet Photoelectron Spectroscopy (UPS) was performed by PHI 5000 VersaProbe III with He I source (21.22 eV) under an applied negative bias of 9.0 V. X-ray photoelectron spectroscopy (XPS) was performed by PHI 5000 VersaProbe III with a monochromatic Al  $K\alpha$  X-ray source with the beam size of 200  $\mu\text{m}$ . Charge compensation was achieved by the dual beam charge neutralization and the binding energy was corrected by setting the binding energy of the hydrocarbon C 1s feature to 284.8 eV. The curve fitting was performed by PHI MultiPak software, and Gaussian-Lorentz functions and Shirley background were used. Electron probe microanalysis (EPMA) was performed by EPMA-1720.

## Support figures and table

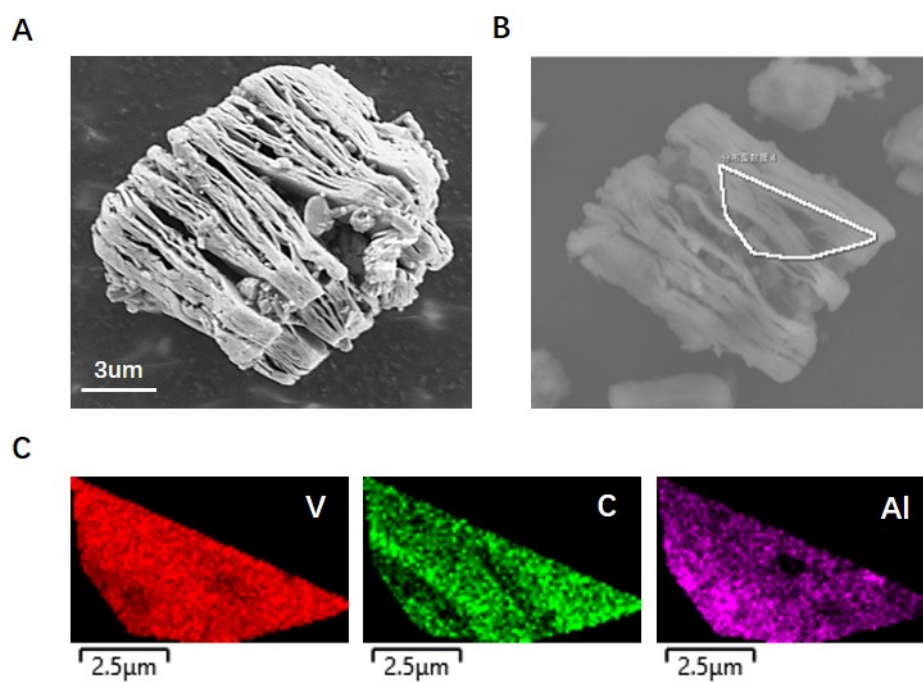


**Figure S1.** (A) SEM images of  $V_2CT_x$  nanosheets. (B) and (C) EDX elemental mapping of  $V_2CT_x$  nanosheets.

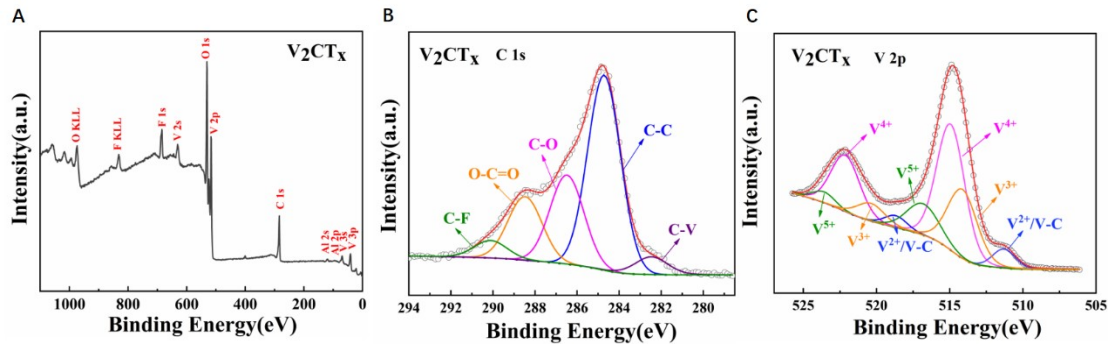


**Figure S2.** (A) The XPS spectra of  $V_2CT_x$  MXene. ((B) and (C)) High-resolution spectra of C 1s and V 2p.

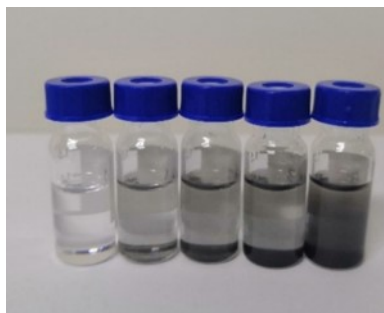


**Figure S3.** The images of CB solution and  $V_2CT_x$ -CB solution with different concentrations of  $V_2CT_x$  (0.005mg/mL, 0.01mg/mL, 0.015mg/mL and 0.02mg/mL) from left to right.

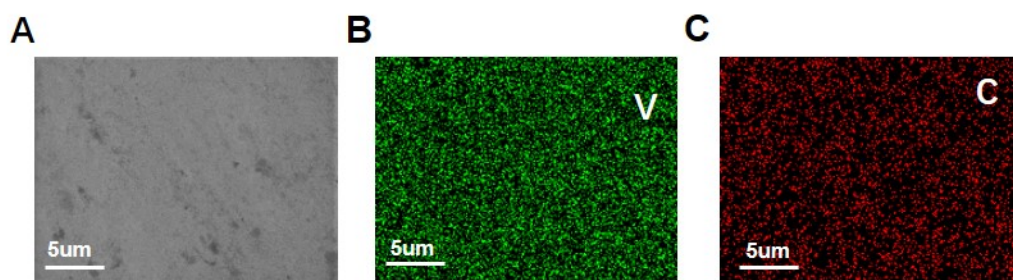


**Figure S4.** (A) The SEM images and (B-C) EDS elemental mapping of V and C distribution in the film of  $V_2CT_x$ -CB deposited on ITO substrates.

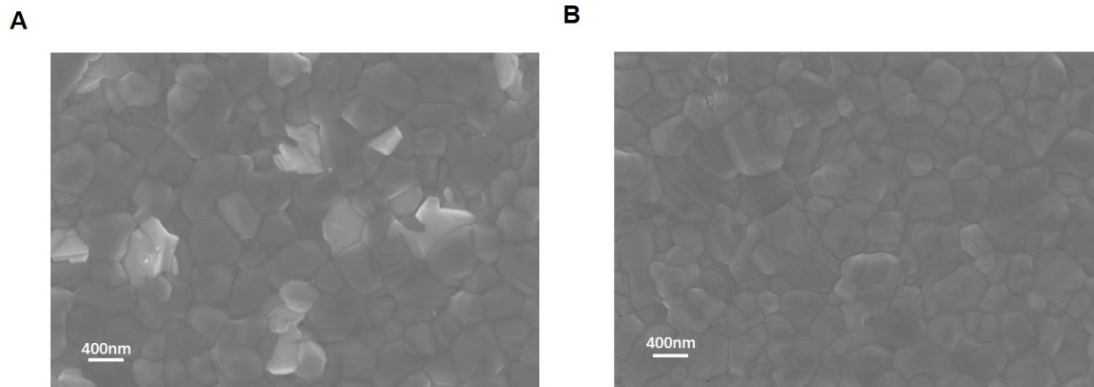


**Figure S5.** SEM images of (A) control perovskite film (0 mg/mL  $V_2CT_x$ ) and (B) target perovskite film (0.01 mg/mL  $V_2CT_x$ ).

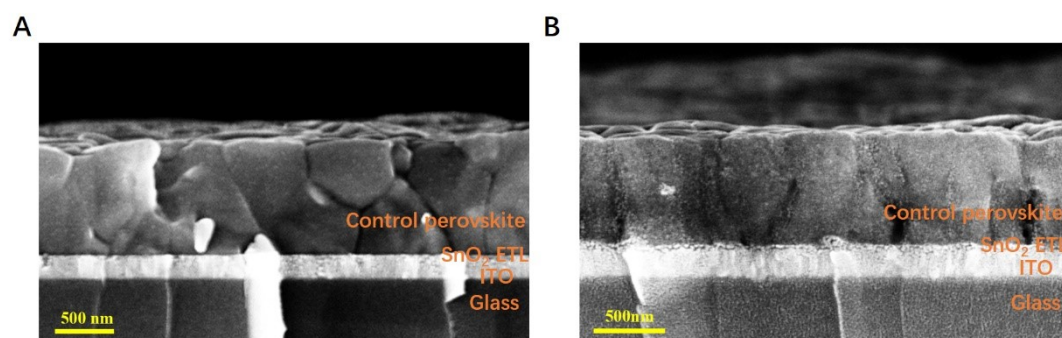


**Figure S6.** Cross-sectional SEM images of (A) control and (B) target perovskite films on SnO<sub>2</sub> ETL.

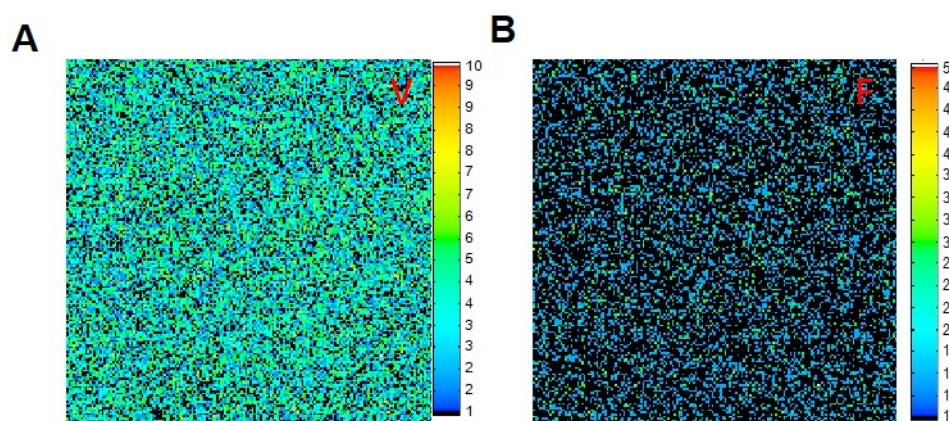


**Figure S7.** EPMA elemental mapping for V and F, scanning kelvin probe microscopy image for target film on SnO<sub>2</sub> substrates.



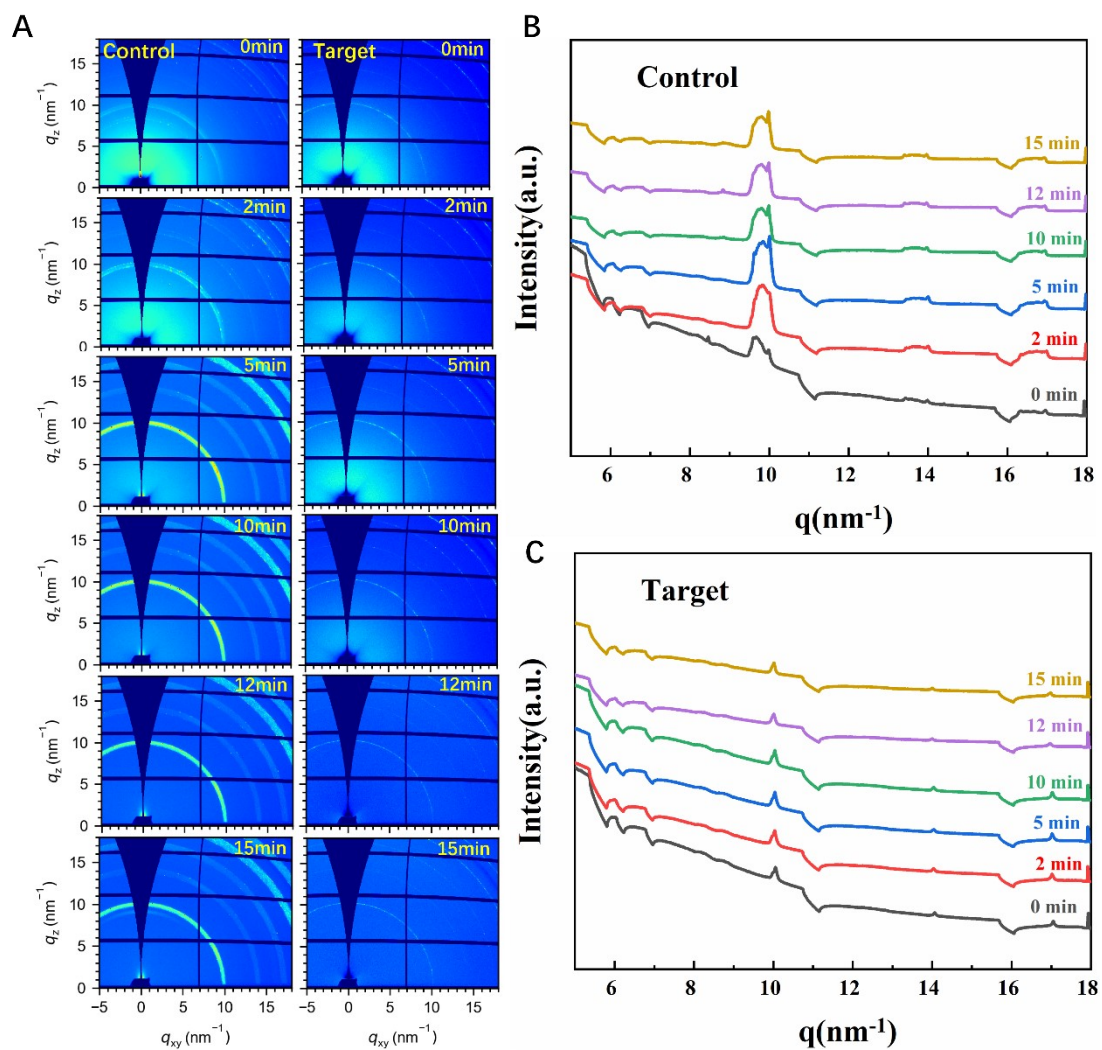


**Figure S8.** *In-situ* GIXRD measurement for the annealing stage of control and target perovskite films.

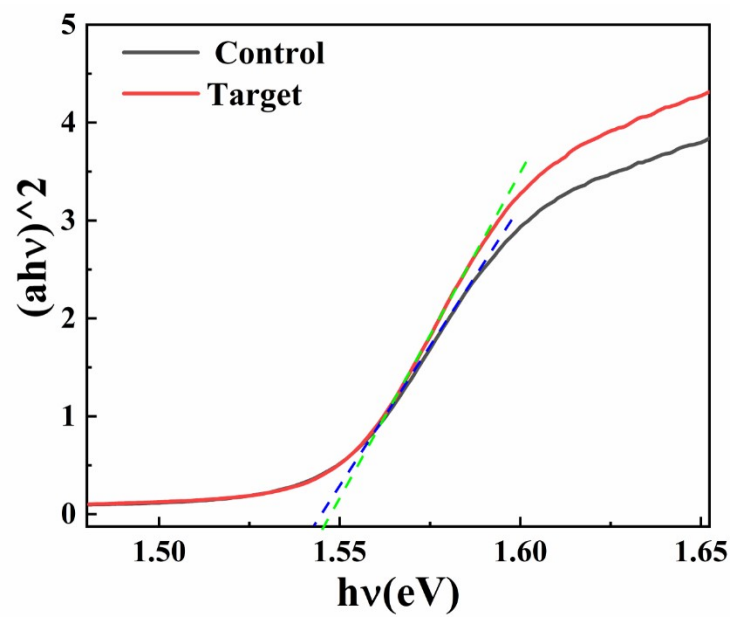


**Figure S9.** Tauc plot of control and target perovskite films.

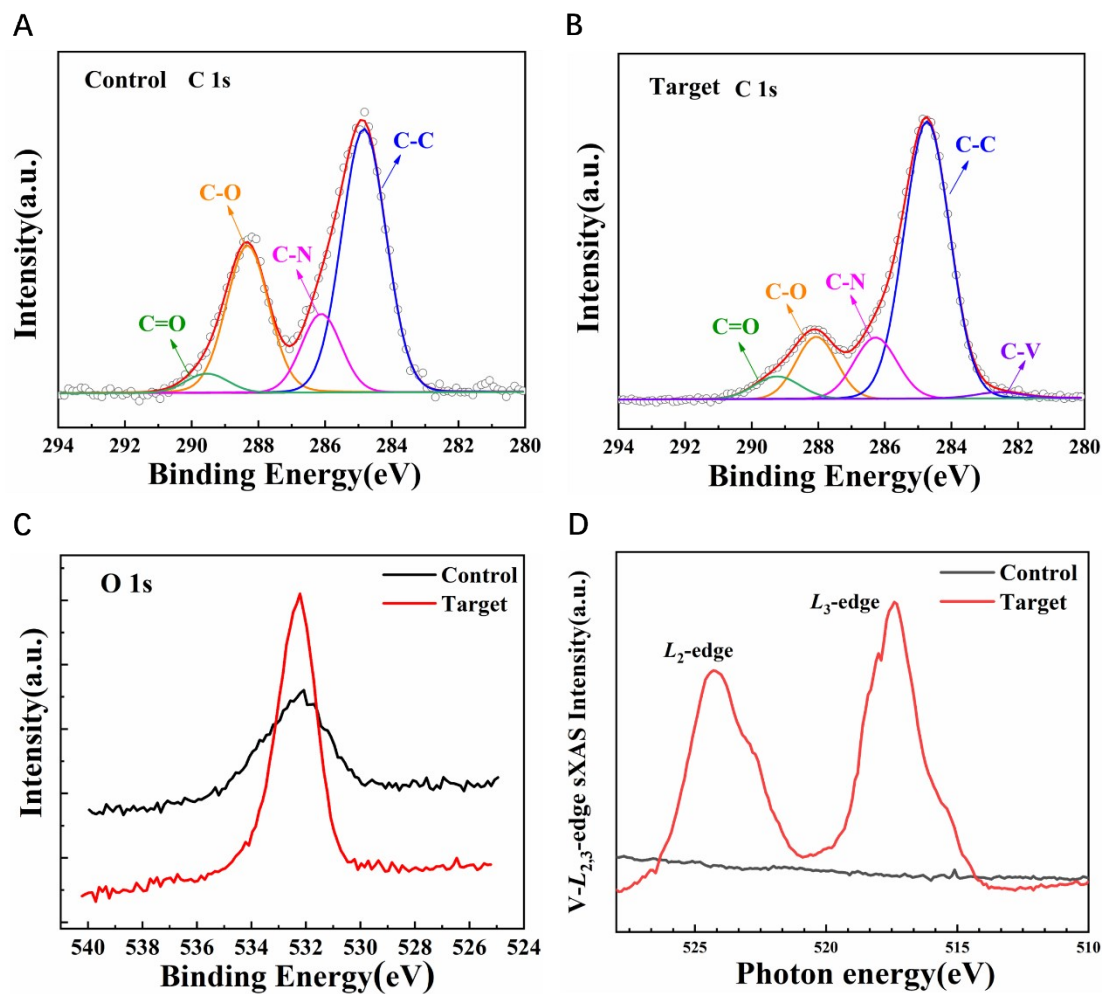


**Figure S10.** XPS of (A-B) C 1s and (C) O 1s from control perovskite film and target perovskite film. (D) V  $L_{2,3}$ -edge sXAS spectra collected on control and target perovskite film.

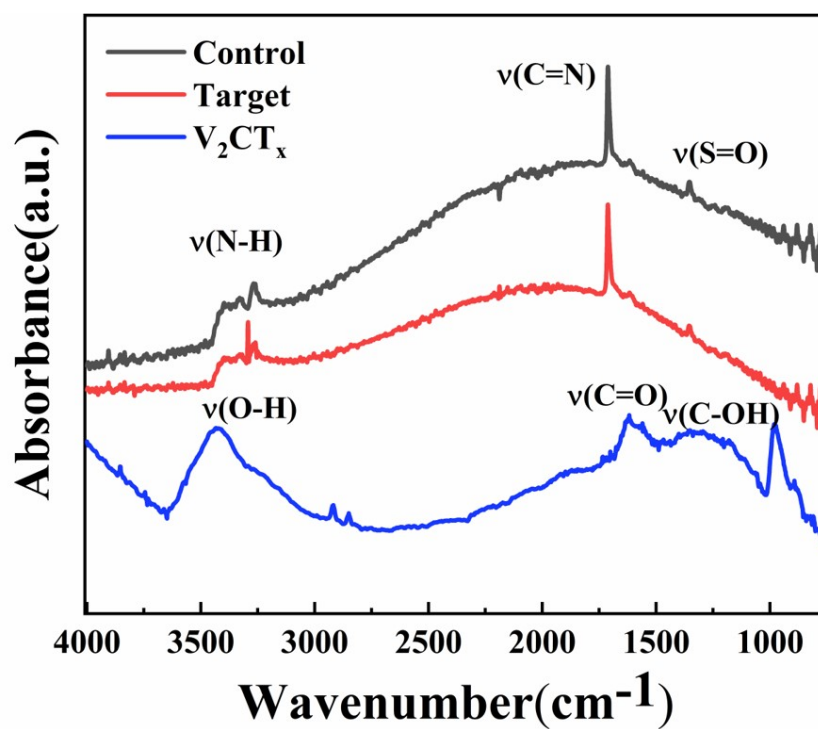


**Figure S11.** IR spectra of control perovskite film, target perovskite film and V<sub>2</sub>CT<sub>x</sub> MXene.

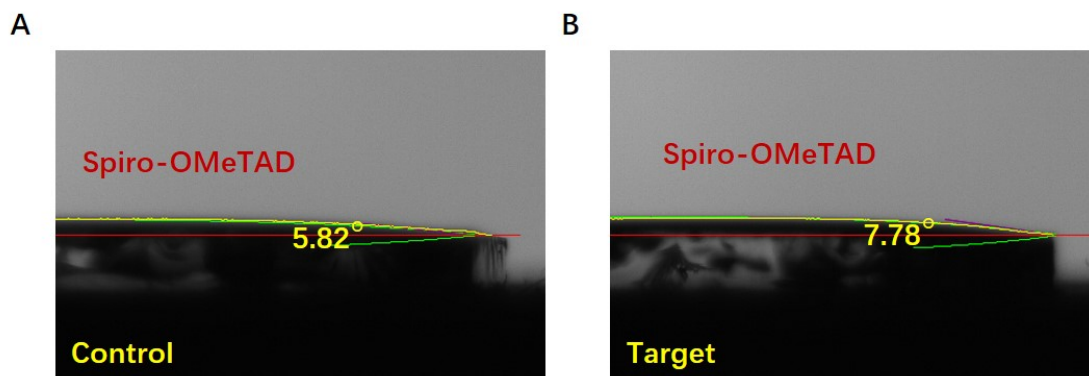


**Figure S12.** The images of Spiro-OMeTAD droplet contact angles on (A) control perovskite film and (B) target perovskite film on SnO<sub>2</sub> surfaces.

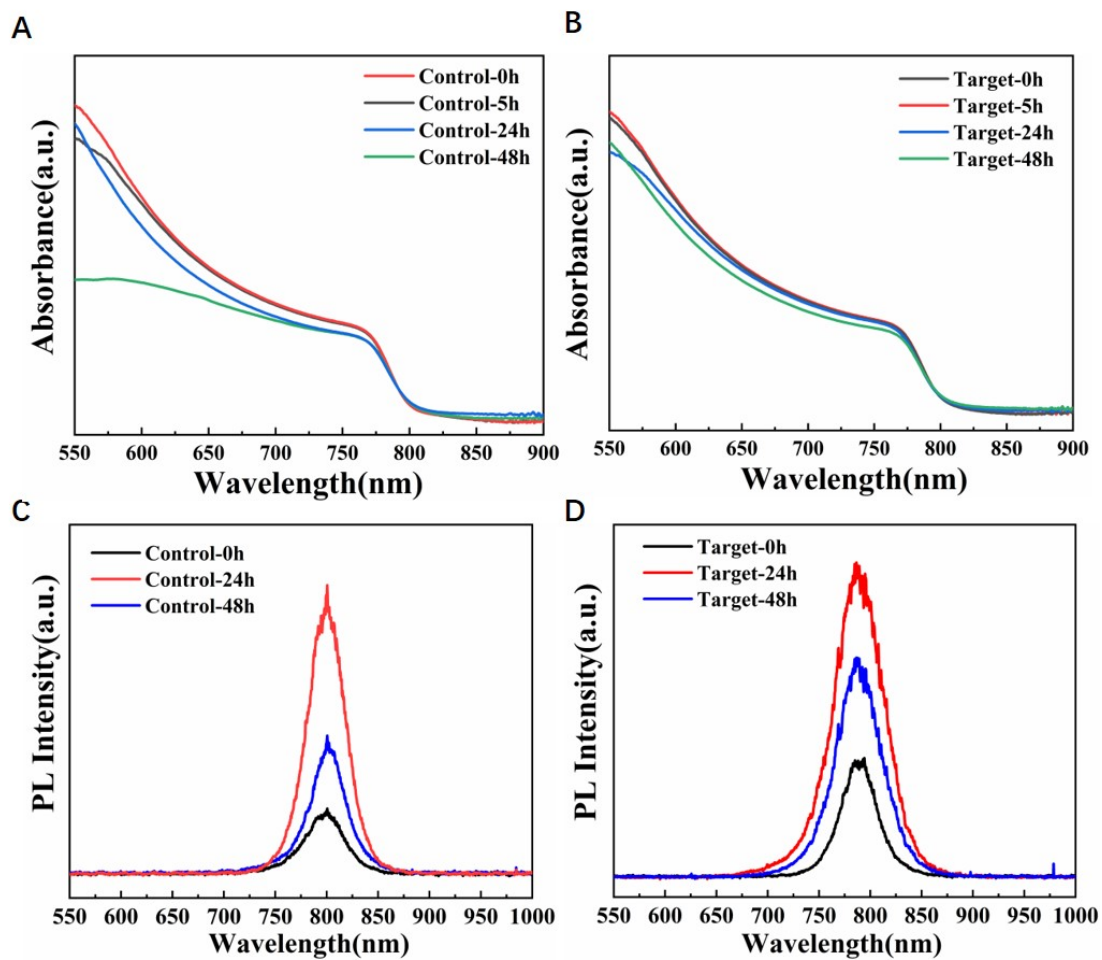


**Figure S13.** The(A-B) UV-vis absorption spectra and (C-D) steady-state PL spectra of the control and target films exposure under 60-70% environmental humidity at 100°C under the ambient air for 48 h.

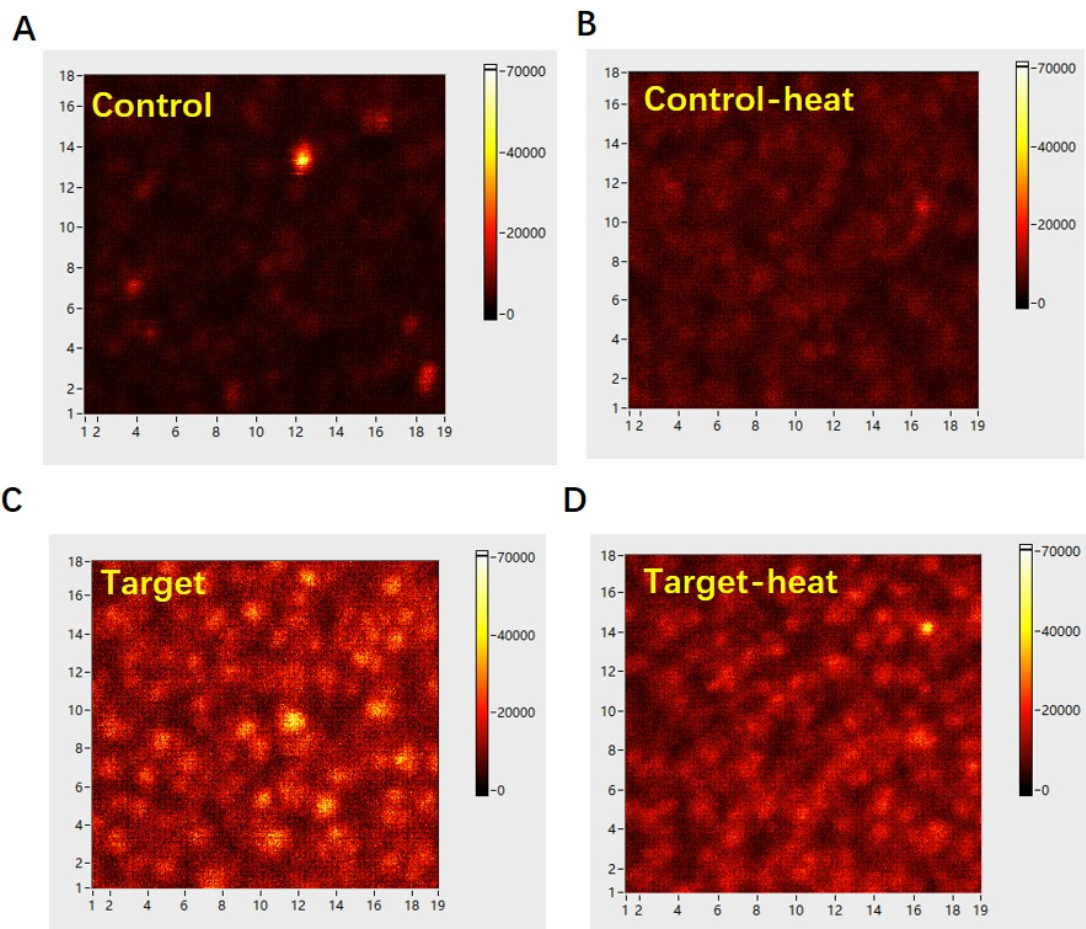


**Figure S14.** The PL mapping of the (A-B) control and (C-D) target films heated at 100°C under the ambient air for 2 h.

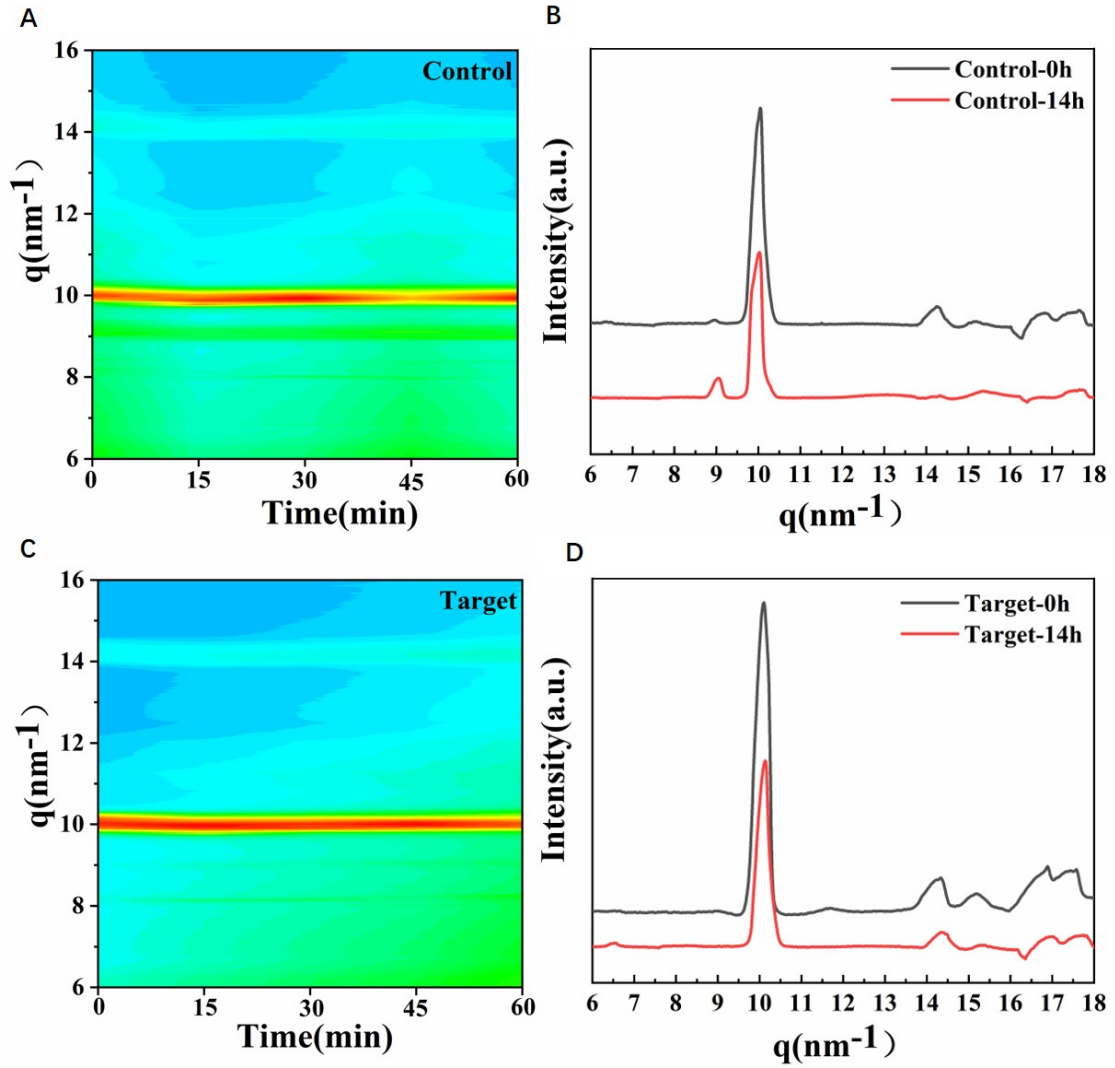


**Figure S15.** (A and C) *In-situ* GIXRD measurements on the thermal stability of perovskite films. The integrated 1D-GIXRD spectra of control (A) and target (C) perovskite films heated at 100 °C in an ambient environment with 50-70% relative humidity for different times. The integrated 1D-GIXRD spectra of control (B) and target (D) perovskite films in an ambient environment with 30-50% relative humidity for 0h and 14h.

**Table S1.** Fitting parameters for the time-resolved PL curves of perovskite films on ITO substrates.

Samples	$\tau_{ave}(ns)$	$\tau_1(ns)$	$\tau_2(ns)$	$A_1(\%)$	$A_2(\%)$
Control	288.52	17.42	339.52	0.55	0.15
Target	1000.93	35.12	1064.65	0.5	0.25